Journal of Glaciology, Vol. 46, *No.* 155, 2000

Analysis of a 3 year meteorological record from the ablation zone of Morteratschgletscher, Switzerland: energy and mass balance

J. Oerlemans
Institute for Marine and Atmospheric Research, Utrecht University, Princetonplein 5, 3584 CC Utrecht, The Netherlands

ABSTRACT. Since 1 October 1995, an automatic weather station has been operated on the tongue of Morteratschgletscher, Switzerland. The station stands freely on the ice, and sinks with the melting glacier surface. It is located at 2100 m a.s.l., and measures air temperature, wind speed and direction, incoming and reflected solar radiation, pressure and snow temperature. A sonic ranger, mounted to stakes drilled into the ice, measures surface height from which melt rates and snow accumulation can be derived. In this paper the data for the period 1 October 1995 to 30 September 1998 are used to evaluate the surface energy balance. The turbulent energy fluxes are calculated with the bulk method. The turbulent exchange coefficient C_h is used as a control parameter. With $C_h = 0.00127$ the calculated melt equals the observed melt, which is 17.70 m w.e. over the 3 years. When averaged over the time when melting occurs (i.e. 35% of the time), the mean surface heat flux equals 191 W m^{-2}. Net shortwave radiation contributes 177 W m^{-2}, net longwave radiation -25 W m^{-2}, the sensible-heat flux 31 W m^{-2} and the latent-heat flux 8 W m^{-2}.

INTRODUCTION

In recent years, numerical models have been used more and more to study the properties of individual glaciers and ice caps, understand their fluctuations in historic time, and make projections of future behaviour for imposed climate scenarios (e.g. Gregory and Oerlemans, 1998; Oerlemans and others, 1998). Such models have basically two components: an *ice-flow model*, calculating a glacier's changing geometry in response to a changing forcing, and a *mass-balance model*, translating meteorological conditions into glacier mass balance. The general experience from numerical studies is that uncertainties in the mass-balance model are strongly reflected in the output. Consequently, it makes no sense to refine the description of ice flow without a better treatment of the mass balance.

A general problem in testing and calibrating mass-balance models is the paucity of meteorological data from glaciers. In fact, the first question to be answered is how the atmospheric boundary layer overlying a glacier filters the large-scale climatic signal. Especially when the glacier surface is melting and the air is warm, a boundary layer with special properties is present (e.g. Munro, 1989; Van den Broeke and others, 1994; Greuell and others, 1997). Although a number of energy-balance studies have been performed on glaciers (for a review, see Hock, in press), most of these were restricted to one site and covered only a short period.

To obtain a more comprehensive dataset for investigating the boundary-layer structure and its effect on the mass balance, the Institute for Marine and Atmospheric Research, Utrecht University (IMAU), has conducted a number of detailed meteorological field studies in collaboration with other research organizations. These studies aimed to achieve a better spatial and altitudinal resolution, employing many weather stations at the same time (e.g. Oerlemans and Vugts, 1993; Greuell and others, 1995; Oerlemans and others, 1998, 1999). Analysis of the datasets obtained has certainly led to a more complete picture of the physical processes that determine the energy balance of a melting ice/snow surface. Nevertheless, it is clear that longer series of measurements from glacier tongues are also needed. Especially on larger glaciers with large mass turnover, melting on the lower parts is not restricted to the summer and one would like to know what the micrometeorological conditions look like in the other seasons. However, this can only be achieved by using automatic weather stations (AWSs).

On the Greenland and Antarctic ice sheets AWSs have been used over many years and have delivered valuable datasets (e.g. Stearns and others, 1993; Reijmer and others, 1999). However, all of these have been operated close to or above the equilibrium line. Using AWSs in the lower parts of ablation zones for longer periods of time poses different problems. When melt rates are high, constructions drilled into the ice melt out quickly. One solution to this problem is to use stations that stand freely on the ice and sink with the melting surface.

At the IMAU, weather stations have been developed that can operate in an ablation zone unattended for a considerable period of time. The quality of the data collected will generally be less than that of manned stations, but experience has shown that very useful information about the basic meteorological quantities can be obtained. AWSs in melting zones are currently operated in West Greenland, on Vatnajökull, Iceland, and on Morteratschgletscher, Switzerland.

In this paper a 3 year record from the station on Morteratschgletscher is analyzed. An attempt is made to evaluate the surface energy balance. This involves the use of parameterizations to calculate longwave radiation and turbulent

https://doi.org/10.3189/172756500781832657 Published online by Cambridge University Press

exchange. For clouds and longwave radiation the procedure developed by Greuell and others (1997) is applied. Simple bulk equations are used to compute the sensible- and latent-heat flux. The turbulent exchange coefficient appearing in these equations is optimized to make the total calculated melt over the 3 year period equal to the observed melt. In fact, the determination of a turbulent exchange coefficient by closing the energy budget can be regarded as an alternative to profile measurements (and analysis) (e.g. Kuhn, 1979). An extensive study of this method for a 55 day period was made by Hay and Fitzharris (1988). The data from the AWS on Morteratschgletscher now allow the application of the same principle to a much longer period of time.

THE AWS

The AWS (Fig. 1) is located on the tongue of Morteratschgletscher, about 500 m from the glacier snout at 2104 m a.s.l. (as obtained from global positioning system measurements on 29 September 1995). It is placed on a rather homogeneous part of the glacier which slopes gradually (about 5°) towards the north.

The AWS stands freely on the ice, and sinks with the melting surface. The distance between sensors and surface, 3.5 m, thus remains approximately constant when snow cover is absent. In winter the height of the sensors is 3.5 m minus the snow depth at the AWS site. In the 3 years considered in this paper the maximum snow depth was only about 1.2 m. So the height of the sensors varied between 2.3 and 3.5 m. It should be noted, however, that the sensor height is effectively constant for 95% of the time that significant melting occurs.

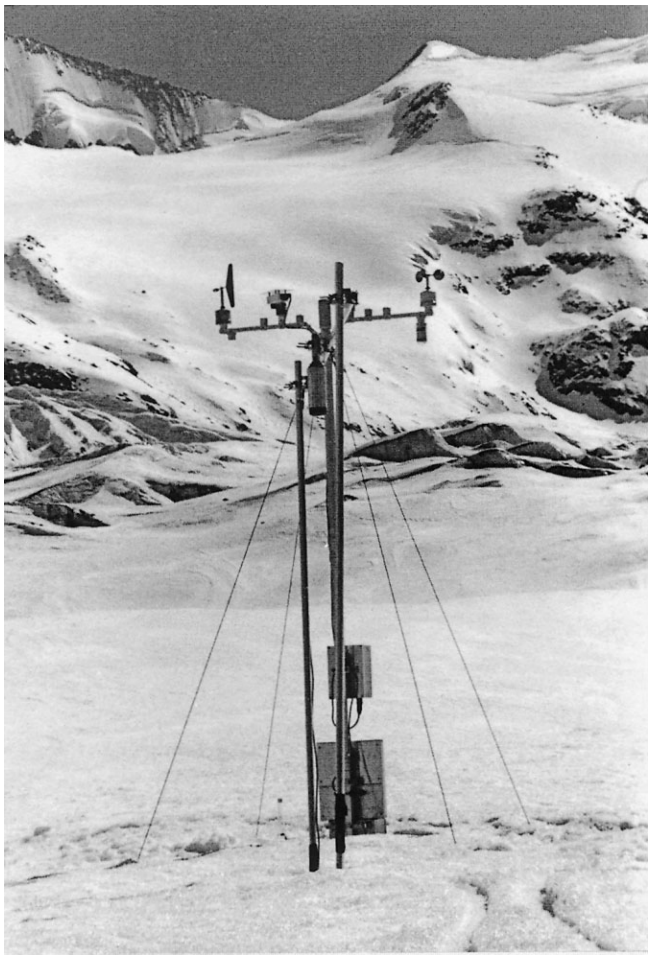

Fig. 1. The AWS on Morteratschgletscher, looking upstream (south). The altitude is about 2100 m. The peak in the middle, at a distance of about 5 km, is part of Bellavista (≈3900 m). The weather station stands freely on the ice; the four legs cannot be seen because they are buried by snow. A solar panel and logger are mounted on the station. In front of the weather station is the sonic ranger, attached to a horizontal rod (barely visible) supported by two stakes drilled into the ice. Photograph taken by the author in April 1997.

The AWS was equipped with sensors for temperature (Aanderaa 2775C, with an aspirator mounted to it), air pressure (Campbell PTA 427A), wind speed (Aanderaa 2740) and wind direction (Aanderaa 2750), and with upward- and downward-looking pyranometers (Aanderaa 2770). Snow temperatures were also measured (Campbell 1D7 probes). Data were sampled every 2 min and then converted into half-hourly mean values and stored on a Campbell CR10 data logger. Power was supplied by a solar panel and lithium batteries. A sonic ranger (Campbell SR-50) mounted on a separate construction drilled into the ice was used to measure the relative surface height. From the data of the sonic ranger snow depth and ice melt can thus be derived. On average the AWS was visited every 10 weeks. During these visits stake readings were carried out at three sites around the station. Measurements with other instruments were done to test and calibrate the sensors on the AWS. For more detail the reader is referred to the field reports (available from the author on request) and Oerlemans and Knap (1998).

Altogether, the AWS has provided a unique 3 year dataset on meteorological quantities, snow accumulation and melt rates, without any significant gaps.

THE DATA

The data used to evaluate the energy balance are summarized in Figure 2. Daily averages are shown, although the energy-balance calculation is based on half-hourly averages. At the top, wind speed is shown. Generally speaking, wind speeds are low: the 3 year mean value is 3.0 m s^{-1} and daily mean values never exceed 7 m s^{-1}. There is no marked seasonal cycle.

Daily mean values of air temperature are shown in the second panel. At 3.5 m above the glacier surface, the annual range is typically 14 K. The annual mean temperature is 1.5 K. It can also be seen that the daily mean temperature on the warmest days in winter is comparable to that of the coldest days in summer.

The third panel shows global radiation. It is interesting to see how the day-to-day variability increases in spring. This feature seems to be related to the disappearance of snow on the sides of the valley, reducing the effect of multiple reflection over the glacier. The mean global radiation is 145 W m^{-2}. A comparison with the annual mean extra-terrestrial irradiance, 292 W m^{-2}, makes clear that shading and clouds strongly reduce the amount of solar energy impinging on the glacier surface. With a mean albedo of 0.55, this implies that only about one-quarter of the solar energy available at the "top of the atmosphere" is absorbed at the glacier surface. Albedo exhibits a marked seasonal cycle, which is related to the albedo difference between ice and snow. A characteristic value in winter is 0.7, in summer 0.35. Snowfall events show up as distinct peaks in the record.

Snow depth as obtained with the sonic ranger shows a large difference between the years. Most of this can be attributed to the large amount of snow (1.2 m) falling within

https://doi.org/10.3189/172756500781832657 Published online by Cambridge University Press

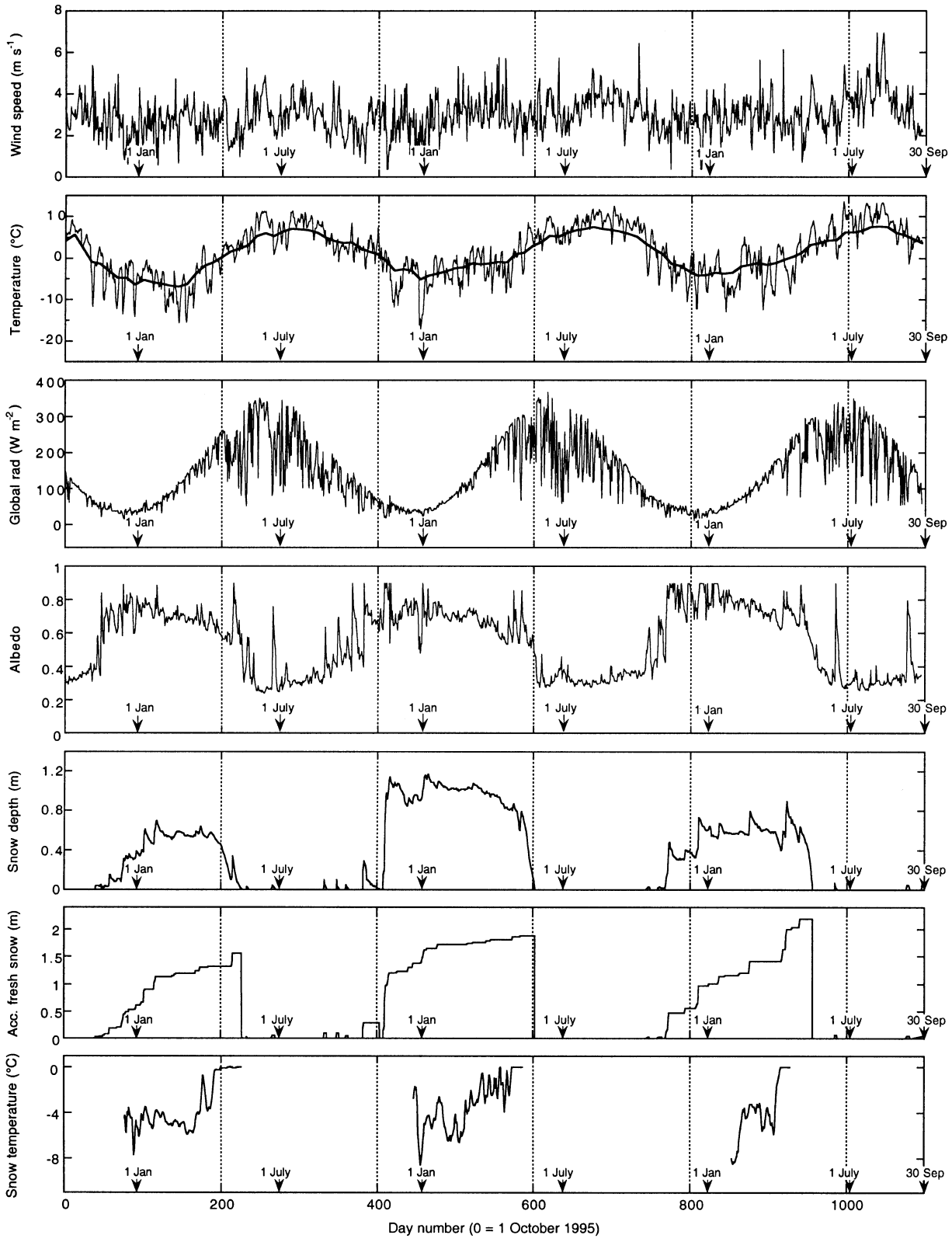

Fig. 2. Data used in this study. Shown are daily mean values of wind speed, air temperature, global radiation, albedo, snow depth, accumulated fresh snow and mean temperature of the snowpack for the entire 3 year period, 1 October 1995 to 30 September 1998.

2 days at the beginning of the second winter. In the cold weather that followed, densification of the snowpack was slow. Interestingly, the third year had the largest total amount of fresh snow, so the record shows no relation between mean snow depth and total snow accumulation.

Finally, the mean temperature of the snowpack is shown. This temperature is estimated from four sensors, or fewer when some of the data appeared unreliable (e.g. when the upper sensors melt out). The mean snow temperature is not used in the calculations, except for the dates at which the snowpack has been heated up to the melting point and run-off may start.

In July 1998 a second station was placed only a few metres away. This had some additional sensors, for humidity and longwave radiation. Data from these sensors for the period 9 July–30 September 1998 could be used to check the parameterization of the incoming longwave radiation, as described later.

To validate the energy-balance calculation a curve is needed that gives the ablation in water equivalent for the

https://doi.org/10.3189/172756500781832657 Published online by Cambridge University Press

entire period. This curve consists of daily values. Ablation of ice is simply calculated from the lowering of the ice surface, assuming a mean ice density of 900 kg m^{-3}. To this is added the ablation in the form of melted snow. It is assumed that runoff can only occur when the mean snow temperature has reached the melting point (see bottom panel in Fig. 2). Between this moment and the disappearance of the snow there is no daily information on the actual amount of melt. Therefore the melt of the snowpack appears as a step in the ablation curve on the day when all snow has disappeared.

To convert accumulated fresh snow into water equivalent, a density of 180 kg m^{-3} has been used. This gives the best fit to the data obtained from snow pits (on 16 December 1995, 19 February 1996, 18 March 1996, 18 April 1996, 19 December 1996, 6 February 1997, 26 February 1997 and 18 April 1997). The resulting ablation curve is shown in Figure 3, together with the measured surface height.

CALCULATION OF THE ENERGY BALANCE AND ABLATION

The energy flux at the surface F is calculated as

$$F = S_{\mathrm{in}} + S_{\mathrm{out}} + L_{\mathrm{in}} + L_{\mathrm{out}} + H_{\mathrm{se}} + H_{\mathrm{la}}\,, \qquad (1)$$

where S_{in}, S_{out}, L_{in} and L_{out} are the incoming and outgoing fluxes of shortwave and longwave radiation, respectively. H_{se} is the sensible-heat flux and H_{la} the latent-heat flux. Conduction into the ice or snow is neglected, although heating of the snow by meltwater in spring is taken into account as discussed in the previous section. Fluxes towards the surface are considered positive.

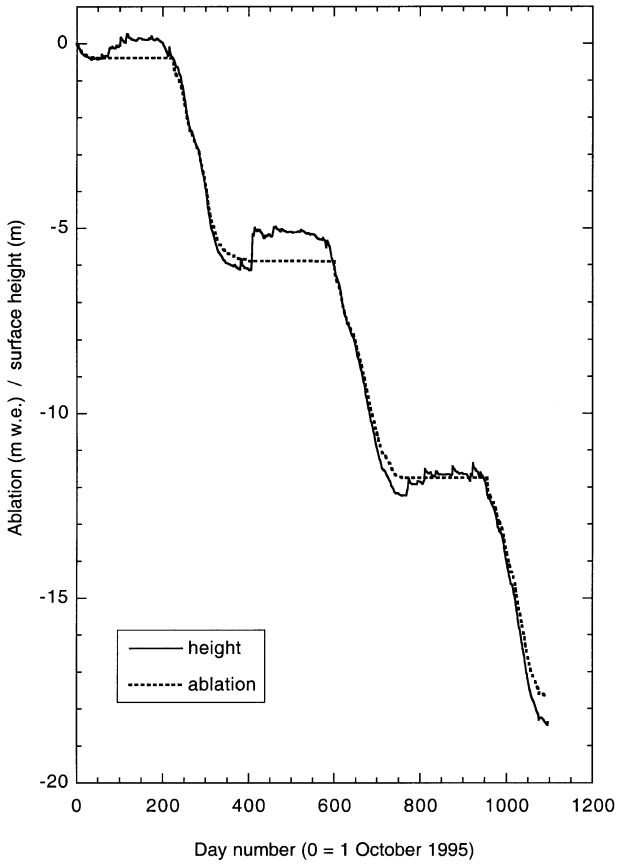

Fig. 3. Measured surface height and total ablation curve for the 3 year period.

The mass-balance equation reads

$$\dot{M} = -\frac{F}{L_{\mathrm{m}}} + \frac{H_{\mathrm{la}}}{L_{\mathrm{v}}}\,, \qquad (2)$$

where $\dot{M}$ is the rate of change of mass, L_{m} is the latent heat of melting and L_{v} is the latent heat of vapourization. The first term on the righthand side describes the runoff due to melting. It is assumed that melting occurs as soon as $F > 0$. Meltwater runs off immediately unless the snowpack has a temperature below the freezing point. The last term in Equation (2) describes the mass exchange between surface and atmosphere associated with the latent-heat flux. It is not known a priori if the latent-heat flux involves an ice-to-vapour or water-to-vapour phase transition. Here the latent heat of vapourization is used as an arbitrary choice.

The data from the AWS do not allow evaluation of the energy fluxes with the accuracy normally obtained with a manned energy-balance station at which profile and/or turbulence measurements are also carried out. Therefore a pragmatic approach will be taken in which a control parameter (turbulent exchange coefficient for sensible and latent heat C_{h}) is optimized in such a way that the calculated melt over the 3 year period equals the observed melt. In fact, determination of C_{h} from direct meteorological observations (profile measurements) on a glacier surface is sometimes problematic (e.g. Oerlemans, 1998) and methods in which C_{h} is determined from a closure of the long-term energy budget provide a useful alternative (e.g. Kuhn, 1979).

RADIATION

The radiation sensors on the AWS were approximately parallel to the glacier surface (in the 3 years considered, the tilt of the weather station was 4–8° to the north to north-northeast). The measurements thus provide the best estimate of the amount of solar radiation available at the glacier–atmosphere interface. Although global radiation (referring to a horizontal plane) was calculated by taking into account the tilt of the sensors, the actually measured shortwave radiation was used in the evaluation of the surface energy budget.

Longwave radiation was not measured and must be deduced. The incoming longwave radiation will be calculated from air temperature, humidity and cloudiness. The parameterization used was derived by Greuell and others (1997), on the basis of the Pasterze (Austria) dataset (Greuell and others, 1995). We assume that the longwave radiation field is isotropic within the reach of the AWS. This is a reasonable assumption when the slope of the glacier surface is approximately constant over several hundreds of metres. As a consequence, the longwave flux L is evaluated as

$$L = L_{\mathrm{in}} + L_{\mathrm{out}} = L^{*}_{\mathrm{in}} + \varepsilon_{\mathrm{s}}\sigma(T_{\mathrm{s}} + 273.15)^{4}\,, \qquad (3)$$

where L^{*}_{in} is the parameterization of incoming longwave radiation referred to earlier (Greuell and others, 1997). The second term is the outgoing longwave radiation. T_{s} is the surface temperature, σ is the Stefan–Boltzmann constant and ε_{s} is the surface emissivity, assumed to be unity.

The most important predictor in the scheme for incoming longwave radiation is cloudiness. As cloud observations are not available, cloudiness has to be estimated from the record of shortwave radiation. However, it was impossible to do this on an hourly basis. The three-dimensional radiation field in the Morteratsch valley is complicated, especially when the valley walls are covered with snow (multiple reflections

https://doi.org/10.3189/172756500781832657 Published online by Cambridge University Press

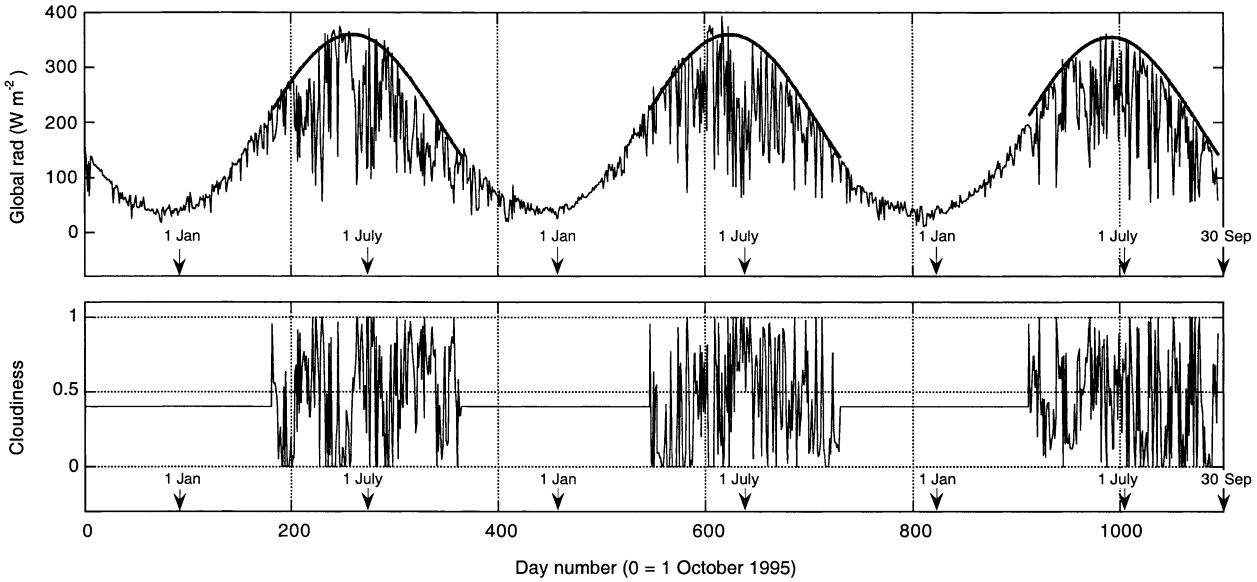

Fig. 4. Upper panel: Clear-sky envelope S_E defined for incoming shortwave radiation (sine functions fitted to the summer half-years). Lower panel: Computed cloudiness.

between clouds, glacier surface and valley walls). As can be seen from the record of daily mean global radiation (Fig. 2), it is very difficult to define a clear-sky envelope for the winter half-year (more precisely: the period of the year when the terrain surrounding the glacier tongue is snow-covered). For the summer half-year this is possible, as shown in Figure 4. The clear-sky envelope S_E, assumed to give the daily mean global radiation when cloudiness is zero, is a simple sine function adjusted to the data.

The reduction of the clear-sky radiation by clouds has been studied in a number of energy-balance studies on glaciers. Here we again use results from the Pasterze experiment (Greuell and others, 1997), because the size and setting of this glacier resembles that of Morteratschgletscher. Greuell and others found a clear relation between atmospheric transmissivity τ_n and cloudiness n of the form:

$$\tau_n = 1 - bn - an^2 , \qquad (4)$$

where a and b are constants ($a = 0.415$ and $b = 0.233$; the resulting curve is shown in Fig. 5). In the present calculation, the transmissivity τ_n is taken as the measured incoming shortwave radiation divided by S_E. Daily mean cloudiness can then be estimated from Equation (4). On days when τ_n as defined above exceeds 1, cloudiness is set to zero. The result is shown in Figure 4 (lower panel). Outside the summer periods for which the calculation has been done, a mean cloudiness of 0.4 is used (the energy-balance calculation is not sensitive to this choice since melting then hardly occurs).

Now half-hourly values of the incoming longwave radiation L_{in} are calculated from the equation given by Greuell and others (1997) from the Pasterze experiment:

$$L_{in} = \left[\varepsilon_{cs}(1 - n^2) + \varepsilon_{ov} n^2\right]\sigma T , \qquad (5)$$

where ε_{cs} and ε_{ov} are the atmospheric emissivities for clear and overcast sky, respectively, and T is air temperature at 2 m in °C. The value of ε_{ov} will be close to one, of course, because clouds block longwave radiation very effectively. The clear-sky emissivity depends on temperature and atmospheric vapour pressure at 2 m according to:

$$\varepsilon_{cs} = 0.23 + 0.475\left(\frac{e_a}{T}\right)^{\frac{1}{8}} \qquad (6)$$

For ε_{ov} Greuell and others (1997) give a value of 0.976 which is also used here.

A few problems remain with regard to this calculation. First of all, humidity has not been measured. Here the relative humidity R is set to a constant value of 0.64 (in accordance with the mean humidity for the period 9 July–30 September 1998 measured at the parallel station). The saturation vapour pressure e_s over water or melting ice can be obtained from

$$e_s = 610.8 \exp\left[19.85\left(1 - \frac{273.15}{T}\right)\right] . \qquad (7)$$

With $e_a = R\, e_s$, the clear-sky emissivity can now be calculated from Equation (6).

Secondly, the air temperature has been measured at a height of >2 m. Denoting the height of the sensor above

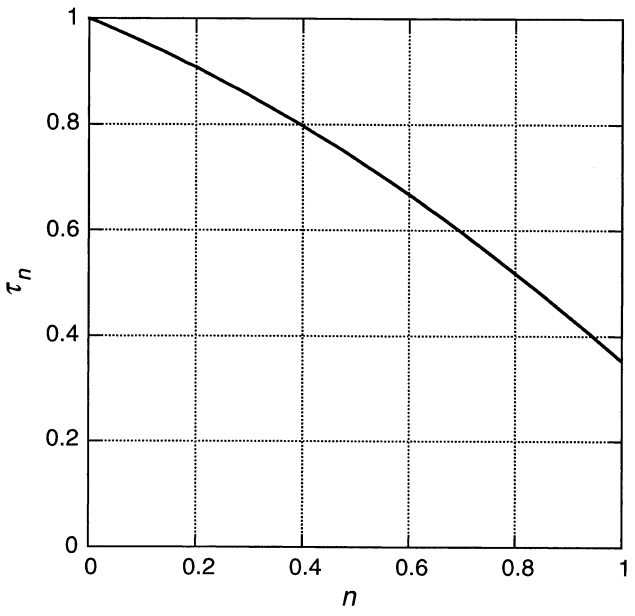

Fig. 5. The relation between daily mean cloudiness (n) and reduction of the global radiation by clouds (τ_n), used to estimate the cloud amount from the measured incoming shortwave radiation.

https://doi.org/10.3189/172756500781832657 Published online by Cambridge University Press

the surface by h, the temperature at 2 m (T_{2m}) is estimated as

$$T_{2m} = \left(\frac{2}{h}\right)^{\mu} T_h \,, \tag{8}$$

where T_h is the temperature in °C at the height h of the sensor (taken as 3.5 m minus the snow depth in m) and μ is a constant. An analysis of the wind and temperature profile measurements carried out on Morteratschgletscher in summer 1997 (personal communication from W. Verbraak, 1997) yields $\mu = 0.162$.

The use of a relation like Equation (8) is only meaningful when the air temperature is above the freezing point. Otherwise the best one can do is to assume that the 2 m temperature is close to the temperature at the height of the sensor. So:

$$\begin{aligned} \mu &= 0.126 \quad \text{if} \quad T_h > 0 \\ \mu &= 0 \qquad \text{if} \quad T_h < 0 \,. \end{aligned} \tag{9}$$

To arrive at the net longwave balance the outgoing radiation must also be calculated. As the surface temperature T_s is unknown it is assumed that

$$T_s = \min(T_h, 0) \quad (\text{in } °C) \,. \tag{10}$$

The parallel station mentioned earlier measures the longwave radiation balance, so it is possible to compare the calculated longwave radiation with the measurements. Although there appear to be significant discrepancies for some days, most likely due to the uncertainty in estimated cloudiness and humidity, the mean value over the period 9 July–30 September 1998 differs by only 3 W m^{-2}.

TURBULENT FLUXES

Because measurements are available for one level only, no attempt was made to use sophisticated schemes for the calculation of the turbulent heat fluxes. Instead the well-known bulk aerodynamic formulas are used:

$$H_s = \rho_a c_p C_h V_{2m} (T_{2m} - T_s) \tag{11}$$

$$H_I = 0.622 \rho_a L_v C_h V_{2m} \frac{(e_{2m} - e_s)}{p} \,, \tag{12}$$

where ρ_a is air density, c_p is specific heat of dry air, C_h is turbulent exchange coefficient, V_{2m} is wind speed at 2 m, T_s is surface temperature, e_{2m} is vapour pressure at 2 m and e_s is vapour pressure at the surface.

For a melting surface $e_s = 610.8$ Pa. For surface temperatures below zero the following expression can be used:

$$e_s = 610.8 \exp\left[22.74\left(\frac{273.15}{T_s} - 1\right)\right] . \tag{13}$$

The wind speed at 2 m is derived from the measurement at sensor height h. The same approach as for temperature is used:

$$V_{2m} = \left(\frac{2}{h}\right)^{\mu} V_h \,. \tag{14}$$

The profile data give $\mu = 0.148$ (cf. the value for temperature: 0.162). Using constant values for air density (1 kg m^{-3}) and pressure (78 500 Pa) the turbulent fluxes can be evaluated if a value for C_h is chosen.

RESULTS

Figure 6 shows the observed and calculated ablation curve for $C_h = 0.00127$. For this value of C_h calculated and

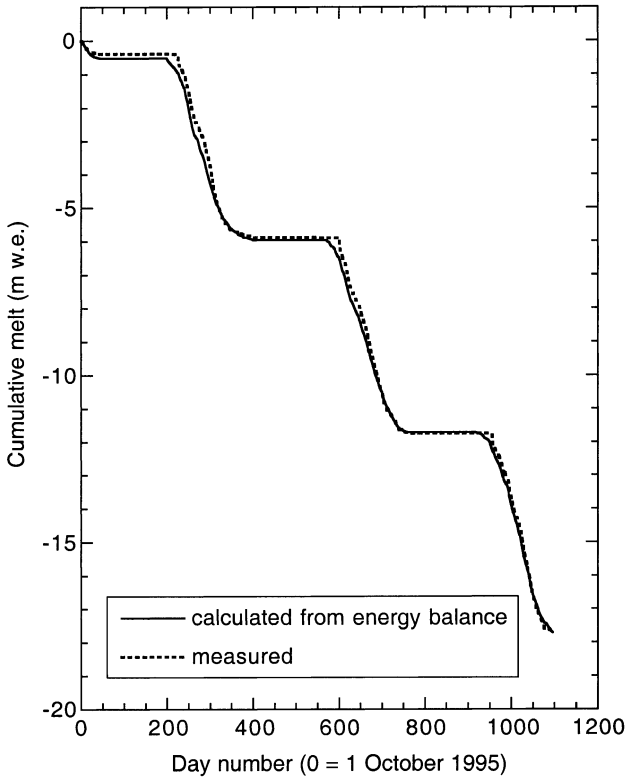

Fig. 6. Observed and calculated melt over the 3 year period. The value for the turbulent exchange coefficient ($C_h = 0.00127$) has been chosen such that the curves coincide at the end.

observed total melt over the 3 years are the same. In the calculation the last term in Equation (2) was ignored for reasons to be discussed later. There is good agreement between calculated and measured melt. The energy-balance calculation slightly overestimates the melt in the first part of the record and underestimates it in the latter part. However, in view of the general errors involved in the measurement of ablation and the radiation budget, the difference between calculated and observed melt is small. In particular, one should realize that the measured change in surface height is a point measurement and not necessarily an accurate estimate of the mass loss in an area of 10 m × 10 m, say (within such an area, differences of several tens of centimetres easily develop within a summer; e.g. Müller and Keeler, 1969).

The corresponding components of the surface energy flux are summarized in Figure 7. Daily mean values are shown. It is noteworthy that, with the optimal value of C_h, the turbulent fluxes are relatively small. It is only on a few warm days in late summer that the turbulent heat flux becomes comparable in magnitude to the net radiation.

The latent-heat flux attains large negative values in winter. It is unclear if this is realistic. It is a direct consequence of the relatively low value of the prescribed humidity in combination with a zero temperature difference between surface and air. However, a run in which all negative latent-heat fluxes were set to zero gives the same melt curve, because a significant negative latent-heat flux occurs only when the total energy flux remains negative. The neglect of the last term in Equation (2) is related to the uncertainties concerning the latent-heat flux in winter. However, the error involved is probably very small. The average latent-heat flux over the 3 years corresponds to a mass loss of about 0.16 m w.e. This is a small value compared to the total mass loss for this period, which is 17.7 m w.e.

The components of the energy balance averaged over all

https://doi.org/10.3189/172756500781832657 Published online by Cambridge University Press

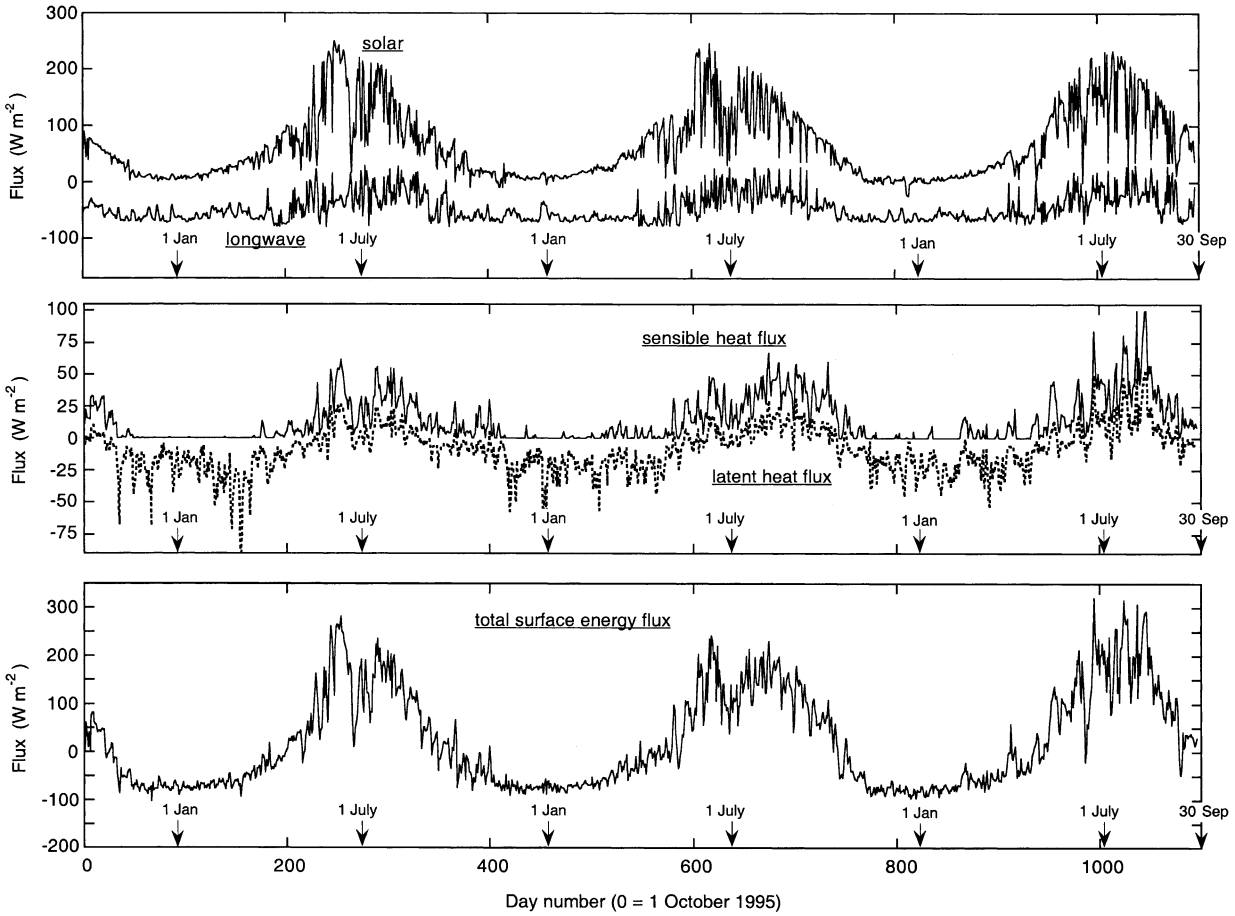

Fig. 7. Components of the calculated surface energy flux, showing daily mean values. Note the differences in vertical scales.

half-hourly periods with a positive surface energy flux are shown in Figure 8. Melt occurs 35% of the time. Again, it is quite clear that shortwave radiation dominates the picture. It is remarkable that, during periods with surface melting, the mean latent-heat flux is positive, i.e. condensation takes place on the glacier surface. The general belief is that this occurs only on the lower parts of maritime glaciers where conditions are very humid. On the lower part of Morteratschgletscher, conditions are not very humid, but are warm. For a 50% relative humidity, condensation occurs when the air temperature exceeds 10°C, which it does on many days. However, the humidity was not measured, but given a constant mean value. Although this value is equal to the mean value obtained from measurements with the new station, the daily cycle is ignored. The relative humidity in the afternoon, when air temperature is highest, could therefore be systematically overestimated.

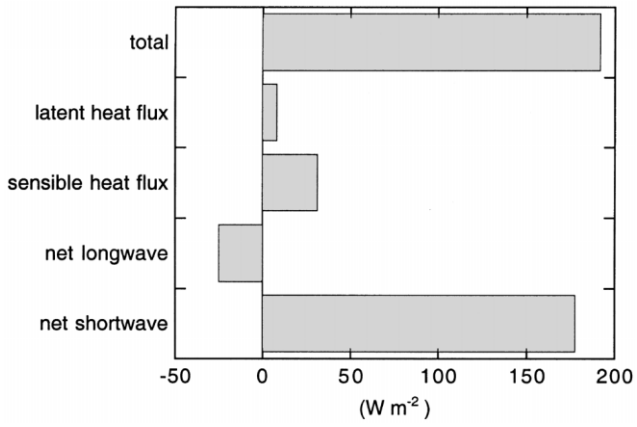

Fig. 8. Components of the surface energy flux averaged over times when there was melting (i.e. about 35% of the time).

Anyway, it appears that the contribution of the latent-heat flux is rather small.

How large is the error in the calculation of C_h? Several factors may contribute to the uncertainty. First of all, the measurement of the ablation is subject to error, as explained above (but it is likely that the relative error decreases when the period of observation is longer). The meteorological observations, especially concerning radiation, suffer from riming and tilting of the mast. However, since the station was visited many times and the tilt of the mast measured, the error may be within 5%. The parameterization of the longwave radiation budget introduces another uncertainty. Although the parameterization was derived from detailed measurements on a glacier, Pasterze, of similar size and in a similar climatic setting, a systematic error is quite possible. In view of this, one may assume that the error in observed melt and net radiation (multiplied by the heat of fusion) is of the order of 1 m w.e. The corresponding error in C_h can be deduced from Figure 9, in which the difference between measured and calculated melt is shown as a function of C_h. The result is: $C_h = 0.00127 \pm 0.00030$.

Putting C_h equal to zero decreases the calculated melt by 3.6 m w.e. over the 3 year period. This corresponds to about 20% of the total melt, in line with the results shown in Figure 8. Figure 9 also shows that a larger exchange coefficient implies a larger fraction of time with surface melting, which would be expected.

COMPARISON WITH OTHER STUDIES

A number of energy-balance studies have been carried out on glaciers, and a comparison of the present results with

https://doi.org/10.3189/172756500781832657 Published online by Cambridge University Press

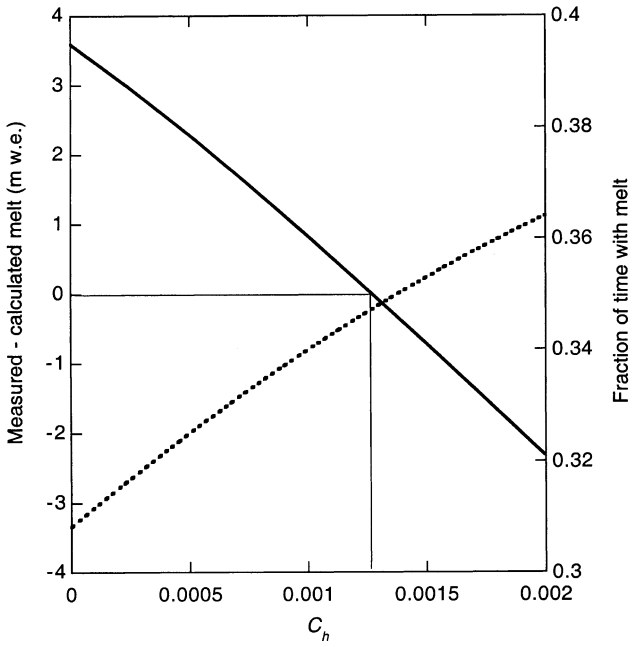

Fig. 9. Calculated melt (solid curve) and fraction of time with melting (dashed curve) as a function of the turbulent exchange coefficient C_h.

earlier findings is in order. Unfortunately, many studies have been of very short duration (for a review, see Hock, in press). Another complicating factor is the different treatment of the turbulent fluxes in the various studies. Bulk equations sometimes are used with a prescribed roughness length taken from other studies. Clearly, these are not useful for the purpose of comparison. In other studies roughness lengths as derived from profile analysis are given, but relating these to C_h is straightforward only when the air above the glacier is neutrally stratified, which, during periods with significant turbulent fluxes, is never the case. Moreover, the application of stability corrections in katabatic conditions has a number of problems (Oerlemans, 1998; Denby, 1999; Van der Avoird and Duynkerke, 1999), so no attempt was made to derive exchange coefficients from published roughness lengths. This leaves only a few studies on valley glaciers that cover a reasonably long period (>50 days) and allow a value to be inferred for the exchange coefficients from the published material. These are listed in Table 1.

Apparently, the value for the exchange coefficient derived in the present study is considerably lower than those found by Hogg and others (1982) and particularly Hay and Fitzharris (1988). This can partly be attributed to the difference in sensor height referred to above, since during conditions of melting temperature and wind-speed increase with height, the exchange coefficient will be larger for a smaller sensor height. Equations (8) and (14) can be used to make a first-order correction for the effect of the sensor height, yielding the values shown in italic in Table 1. The value of Hogg and others (1982) is in reasonable agreement with the value found here, while the value of Hay and Fitzharris remains large. The discrepancy may be partly attributed to a difference in the morphology of the glacier surface. In the study of Hay and Fitzharris the glacier surface consisted of bare ice, whereas in the present study and that of Hogg and others there is snow-covered ice as well as bare ice. In general, but not always, one finds smaller exchange coefficients over snow than over (rough) ice.

For the Morteratsch study the surface conditions (snow or bare ice) are known. An attempt was therefore made to use two exchange coefficients, one for snow and one for ice, and to find the best values by minimizing the root-mean-square difference between measured and calculated melt for the entire 3 year period. However, this method did not produce a statistically significant difference between the exchange coefficients over snow and over bare ice.

SENSITIVITY OF MELT TO AIR TEMPERATURE

The sensitivity of glacier mass balance to a change in air temperature has been the subject of many studies, and it is interesting to repeat the energy-balance calculation for the Morteratsch data with a higher or lower air temperature. The most straightforward way is to increase or decrease the temperature at 3.5 m with a constant value through the year. However, the relation between the 3.5 m temperature and the "large-scale temperature" is not simple, because at 3.5 m height the air is still within the thermal influence of the glacier surface.

Air temperature affects the melt rate in two ways: the turbulent heat flux as well as the downward longwave flux are related to it. The dependence of the annual mean melt rate on air temperature is shown in Figure 10. The sensitivity (change in melt rate per degree temperature change) is about 0.36 m w.e. $a^{-1} K^{-1}$. This value can be compared to the sensitivity of the *mean specific balance* for glaciers in a moderately wet climate, for which a value of 0.5 m w.e. $a^{-1} K^{-1}$ is normally taken as a typical value (e.g. as modelled for a number of glaciers by Oerlemans and Fortuin, 1992). The difference can be explained by considering feedbacks. In models that calculate the response of the specific balance to a changing temperature, two mechanisms are included that enhance the sensitivity: albedo feedback, effectively reducing/increasing

Table 1. A comparison with two other energy-balance studies on glaciers

Study	*Location*	*Duration*	C_h
Hogg and others (1982)	Hodges Glacier, South Georgia, Southern Ocean	155 days (summer)	
		[u, T at 1 m]	0.0017
		[$u, T \rightarrow 2$ m]	*0.0014*
Hay and Fitzharris (1988)	Ivory Glacier, New Zealand	155 days (summer)	
		[u, T at 1.2 m]	0.0039
		[$u, T \rightarrow 2$ m]	*0.0033*
This paper	Morteratschgletscher, Switzerland	3 years	0.0013 ± 0.0003
		[u, T at 2 m]	

https://doi.org/10.3189/172756500781832657 Published online by Cambridge University Press

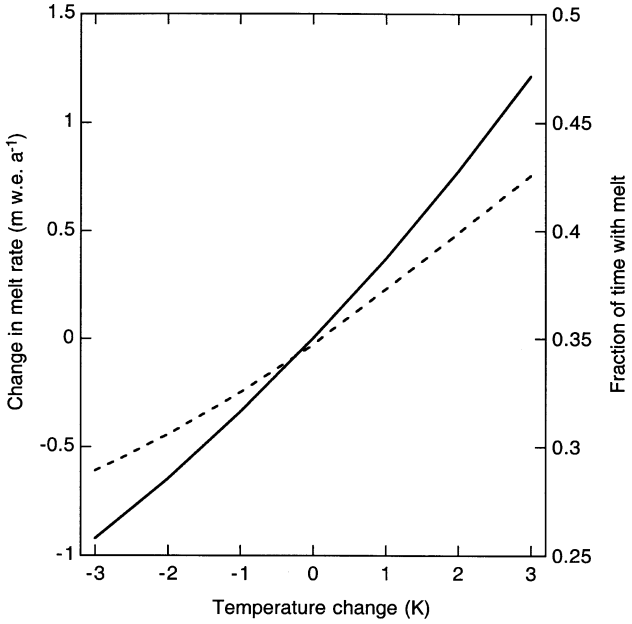

Fig. 10. The relation between the melt rate and air temperature (solid line). The dashed line shows how the fraction of time when melting occurs varies with temperature.

absorption of shortwave radiation for lower/higher temperatures, and solid precipitation feedback, increasing/decreasing the fraction of precipitation that falls as snow for lower/higher temperatures. Such factors are not dealt with in the energy-balance calculation with the Morteratsch data.

EPILOGUE

The AWS on Morteratschgletscher has delivered a unique dataset on the meteorological conditions on a glacier snout. The length of the dataset (3 years) has allowed a study of how the various energy fluxes change in the course of the seasons. The evaluation of the energy balance as discussed in this paper involved a number of assumptions and approximations, particularly concerning the longwave radiation budget and the latent-heat flux. The new station, now in operation for some time, measures all four components of the radiation budget and the relative humidity. A few years from now, therefore, the analysis can be repeated with a more complete dataset. At a higher elevation on the glacier, not too far from the equilibrium line (which is at about 3000 m), a second station has been installed. This will offer the possibility of studying vertical gradients in the components of the energy balance from a long dataset.

Knowledge of the turbulent exchange coefficient over glaciers is of great importance, because this coefficient determines to a large extent the sensitivity of glacier mass balance to temperature change. Although refined theories exist for turbulent transfer in the stable boundary layer, in the author's opinion it has not been proven that these work well in katabatic conditions over glaciers. It seems useful to go back to some of the existing datasets on energy fluxes during glacier melt, and evaluate carefully drag/exchange coefficients without invoking profile analysis, roughness lengths and stability corrections. No doubt a scattered picture will result. Nevertheless, if some systematic relation between exchange coefficient and surface conditions (snow/ice, rough/smooth) exists, it should show up. If it does not, one may wonder if a sophisticated treatment of turbulent transfer in energy/mass-balance modelling makes sense.

ACKNOWLEDGEMENTS

I am grateful to everyone who lent a hand in the field. W. Boot and H. Snellen showed their technical skill in constructing a station that was able to survive on an unstable glacier tongue for more than 3 years. I thank the members of the Ice-and-Climate group at the IMAU, R. Braithwaite and G. Wendler for many constructive remarks and suggestions.

REFERENCES

Denby, B. 1999. Second-order modelling of turbulence in katabatic flows. *Boundary-Layer Meteorol.*, **92**, 67–100.

Gregory, J. M. and J. Oerlemans. 1998. Simulated future sea-level rise due to glacier melt based on regionally and seasonally resolved temperature changes. *Nature*, **391** (6666), 474–476.

Greuell, W., M. R. van den Broeke, W. Knap, C. Reijmer, P. Smeets and I. Struijk. 1995. *PASTEX: a glacio-meteorological experiment on the Pasterze (Austria).* Utrecht, Utrecht University. Institute for Marine and Atmospheric Research; Amsterdam, Vrije Universiteit. Faculty of Earth Sciences. (Field Report.)

Greuell, W., W. H. Knap and P. C. Smeets. 1997. Elevational changes in meteorological variables along a mid-latitude glacier during summer. *J. Geophys. Res.*, **102** (D22), 25,941–25,954.

Hay, J. E. and B. B. Fitzharris. 1988. A comparison of the energy-balance and bulk-aerodynamic approaches for estimating glacier melt. *J. Glaciol.*, **34** (117), 145–153.

Hock, R. In press. Glacier melt and discharge: a review on processes and their modelling. *Water Resour. Res.*

Hogg, I. G. G., J. G. Paren and R. J. Timmis. 1982. Summer heat and ice balances on Hodges Glacier, South Georgia, Falkland Islands Dependencies. *J. Glaciol.*, **28** (99), 221–238.

Kuhn, M. 1979. On the computation of heat transfer coefficients from energy-balance gradients on a glacier. *J. Glaciol.*, **22** (87), 263–272.

Müller, F. and C. M. Keeler. 1969. Errors in short-term ablation measurements on melting ice surfaces. *J. Glaciol.*, **8** (52), 91–105.

Munro, D. S. 1989. Surface roughness and bulk heat transfer on a glacier: comparison with eddy correlation. *J. Glaciol.*, **35** (121), 343–348.

Oerlemans, J. 1998. The atmospheric boundary layer over melting glaciers. *In* Holtslag, A. A. M. and P. G. Duynkerke, *eds. Clear and cloudy boundary layers.* Amsterdam, Royal Netherlands Academy of Arts and Sciences, 129–153. (VNE 48.)

Oerlemans, J. and J. P. F. Fortuin. 1992. Sensitivity of glaciers and small ice caps to greenhouse warming. *Science*, **258** (5079), 115–117.

Oerlemans, J. and W. H. Knap. 1998. A 1 year record of global radiation and albedo in the ablation zone of Morteratschgletscher, Switzerland. *J. Glaciol.*, **44** (147), 231–238.

Oerlemans, J. and H. F. Vugts. 1993. A meteorological experiment in the melting zone of the Greenland ice sheet. *Bull. Am. Meteorol. Soc.*, **74** (3), 355–365.

Oerlemans, J. *and 10 others.* 1998. Modelling the response of glaciers to climate warming. *Climate Dyn.*, **14** (4), 267–274.

Oerlemans, J. *and 7 others.* 1999. Glacio-meteorological investigations on Vatnajökull, Iceland, summer 1996. *Boundary-Layer Meteorol.*, **92**, 3–26.

Reijmer, C., W. Greuell and J. Oerlemans. 1999. The annual cycle of meteorological variables and the surface energy balance on Berkner Island, Antarctica. *Ann. Glaciol.*, **29**, 49–54.

Stearns, C. R., L. M. Keller, G. A. Weidner and M. Sievers. 1993. Monthly mean climatic data for Antarctic automatic weather stations. *In* Bromwich, D. H. and C. R. Stearns, *eds. Antarctic meteorology and climatology: studies based on automatic weather stations.* Washington, DC, American Geophysical Union, 1–21. (Antarctic Research Series 61.)

Van den Broeke, M. R., P. G. Duynkerke and E. A. C. Henneken. 1994. Heat, momentum and moisture budgets of the katabatic layer over the melting zone of the West Greenland ice sheet in summer. *Boundary-Layer Meteorol.*, **71** (4), 393–413.

Van der Avoird, E. and P. G. Duynkerke. 1999. Turbulence in a katabatic flow. Does it resemble turbulence in stable boundary layers over flat surfaces? *Boundary-Layer Meteorol.*, **92**, 39–66.

MS received 29 March 1999 and accepted in revised form 28 June 2000